Hindawi
Advances in Materials Science and Engineering
Volume 2019, Article ID 8404857, 9 pages
https://doi.org/10.1155/2019/8404857

Research Article

Effects of Fabrication Parameters on the Properties of Parts Manufactured with Selective Laser Sintering: Application on Cement-Filled PA12

Abdelrasoul M. Gadelmoula[1,2] **and Saleh A. Aldahash**[1]

[1]*Department of Mechanical and Industrial Engineering, College of Engineering, Majmaah University, Al-Majmaah 11952, Saudi Arabia*
[2]*Department of Mechanical Engineering, Faculty of Engineering, Assiut University, Assiut 71515, Egypt*

Correspondence should be addressed to Abdelrasoul M. Gadelmoula; a.gadelmoula@mu.edu.sa

Received 7 January 2019; Revised 19 February 2019; Accepted 4 March 2019; Published 21 March 2019

Academic Editor: Charles C. Sorrell

Selective laser sintering (SLS) becomes a promising technology for manufacturing complicated objects with small to moderate numbers from a wide range of polymeric and metallic powders. However, the fabrication parameters in the SLS process need to be tailored for each end-use fabricated product. Hence, it becomes extremely important to investigate the effects of fabrication parameters on the mechanical and morphological properties of SLS parts. For this purpose, the present experimental work is devoted to evaluating the effects of some important fabrication parameters, that have not received proper attention in the published literature, on the properties of cement-filled polyamide 12 (PA12) parts manufactured with the SLS technique. The effect of scanning vector length on the tensile, compressive, and flexural strength of manufactured PA12/white cement parts is investigated. Also, the end-of-vector (EOV) effect on the edge geometry of manufactured parts is studied. Moreover, the effect of incident laser power (LP) on the surface quality of fabricated SLS PA12/white cement parts is qualitatively evaluated. The results from this work revealed that the scanning vector length significantly affects the mechanical properties of SLS parts provided that the load is applied along the scanning vector direction. Also, it is noticed that excessive exposure to laser energy at layer edges can deteriorate the part's edge and in some cases can cause localized heating and burning of the part's edge and, eventually, can result in surface microcracks. Finally, the experiments confirmed that increasing the laser power can enhance the surface roughness of manufactured parts; however, excessive increase in laser power causes localized burning and initiation of surface microcracks.

1. Introduction

Selective laser sintering (SLS) process has evolved from a rapid prototyping (RP) technique to a promising manufacturing technology which was recently used widely to produce complicated end-use products with small-to-moderate sizes. The evolution of SLS technology is owed mainly to the competitive marks of machine vendors and the ever increasing number of polymeric and metallic powders that can be processed with this technique [1–3]. The SLS process was first invented by Ross Householder in 1979 and commercialized later after the work of Carl Deckard at the University of Texas at Austin in the late 1980s [4]. SLS process is a layer-by-layer manufacturing technique in which the 3D-CAD file of desired object is transferred to the SLS system. The system then slices the thickness of the object into a number of slices (layers) of predetermined thickness. The powder mixture is fed into the two feed cartridges located at either side of the part build cylinder. Then, a thin layer of powder is spread by means of a roller. The machine head scans the part build area to selectively sinter an area corresponding to the current slice geometry. The build cylinder is then lowered with an increment equal to the prescribed layer thickness and the roller spreads a fresh layer of powder to be sintered. The process is repeated until the whole object is manufactured [5].

Mechanical and morphological properties of parts manufactured with SLS technique are influenced by several fabrication parameters. These parameters can be divided into two main categories: powder-related parameters and machine-related parameters [6]. Hence, the fabrication parameters should be optimized for every powder material in order to obtain object properties as designed. Several studies have been carried out to investigate the effects of fabrication parameters on the mechanical and morphological properties of SLS parts for a wide range of powder materials.

A comprehensive work was carried out by Gibson and Shi [6] to investigate the effects of part build orientation, building height levels, and laser power on the tensile strength and density of manufactured specimens; they reported that both tensile strength and part density are orientation-dependent properties and that manufactured SLS parts with shorter scan vectors can have good mechanical properties. The results were further emphasized after the work of Ajoku et al. [7]. Following the previous studies, Caulfield et al. [8] evaluated the effects of build orientation and energy density on the properties of PA12 parts manufactured with SLS and reported that the studied fabrication parameters affected the geometrical and physical properties of manufactured parts. Additionally, the anisotropy in manufactured SLS polymeric parts was investigated by Cooke et al. [9] who found that SLS parts can possess some isotropic mechanical properties and other orthotropic properties within the same part.

The surface integrity of manufactured SLS parts was the focus of few previous studies. Among these works, Singhal et al. [10] attempted to optimize the part build orientation for better surface roughness and minimum build time. Further work was carried out by Bai et al. [11] who have investigated the tribological properties of MoS_2-filled PA12 manufactured with SLS process and reported that the inclusion of MoS_2 filler could improve the impact properties of SLS parts.

Recently, Aldahash [12] has studied the influence of energy density on the dimensions, density, mechanical properties, and morphology of sintered specimens. Moreover, the fabrication parameters were optimized for maximum values of ultimate tensile strength, compressive strength, and flexural modulus.

Despite the previous important and fruitful research studies on SLS process, some important fabrication parameters have not received much attention in the open literature, such as the scanning vector length and the end-of-vector effect. Therefore, the present experimental work is devoted to investigating the effects of scanning vector length and EOV effect on the mechanical and morphological properties of PA12/white cement composite parts fabricated with SLS process. Moreover, the effect of laser power on the surface integrity of fabricated specimens is to be evaluated. The results from this work are expected to enable manufacturers with SLS technology to appropriately select the fabrication parameters suitable for the desired product properties.

2. Materials and Methods

In the following sections, the steps for manufacturing cement-filled PA12 parts using the SLS technique are described in detail. Also, the operating conditions and testing methods are summarized.

2.1. Powder Preparation. Predetermined amount of Portland white cement is added to the ultrafine PA12 powder supplied by EOS in order to obtain a test specimen with a specific weight fraction of white cement. The mixture is then sifted intensively using a "VORTI-SIV" sifter to avoid agglomeration of particles. In order to obtain a homogeneous powder mixture with uniform colour, the sifted powders are mechanically mixed in a high-speed mixer for at least 20 minutes. The specifications of PA12 and Portland white cement powders are given in Table 1.

2.2. SLS Process of PA12/White Cement Composite. The sifted and homogeneous powder mixture is then fed into the two feed cartridges of the "DTM Sinterstation 2000" machine with the specifications given in Table 2. In order to manufacture the test specimens, the 3D-CAD file of specimen geometry is transferred to the SLS system at which the thickness of the specimen is sliced to a number of layers (slices) of 0.1 mm typical thickness. Then, the laser head scans the powder bed to selectively sinter the areas of part build cylinder that corresponds to the current slice geometry. Upon complete scanning of the layer, a fresh layer of powder mixture is spread over the sintered layer, and the process is repeated until the whole specimen thickness is sintered.

The test specimens were manufactured at different levels of laser power (LP) ranging from 4.5 to 8 watt in order to evaluate the effects of energy density (ED) on the mechanical and morphological properties of manufactured specimens. It is important to mention that the average energy density ED in J/mm^2 represents the incident laser energy per unit area of powder bed and can be calculated as

$$\mathrm{ED} = \frac{\mathrm{LP}}{\mathrm{SS} * \mathrm{LS}}, \tag{1}$$

where LP is the laser power (watt), SS is the scan spacing (mm), and LS is the laser beam speed (mm/s). The operating conditions adopted during the SLS of PA12/white cement composite are given in Table 3.

Finally, the sintered part is removed from the part build cylinder and cleaned manually at first using soft brush and then mechanically to remove any sticking powders. The specimens are then coated with ultrathin film of gold using "Agar Auto Sputter Coater" so as to be prepared for inspection using the scanning electron microscope (SEM) [12].

2.3. Mechanical Testing. Specimens are then tested on "Testomeric M500" machine so as to evaluate its ultimate tensile strength, compressive strength, and flexural modulus.

Table 1: Specifications of PA12 and white cement powders [12].

Powder properties	Portland white cement	PA12
Average grain size (μm)	15	51
Bulk density (g/cm^3)	1.142	0.484
Particle shape	Irregular (more angular)	Irregular (more round)
Melting temperature (°C)	1400	185

Table 2: Specifications of the "DTM Sinterstation 2000" machine [12].

	DTM Sinterstation 2000 system
Process	Selective laser sintering
Laser type	CO_2
Laser power (W)	0–50
Spot size (mm)	0.4
Work volume (mm)	Ø300 × 380 Z
Computer system	Pentium-based Unix system
Power supply	240 VAC, single phase

Table 3: Manufacturing conditions of PA12/white cement composite.

Parameter	Value
Laser power (watt)	4.5–8
Scan speed (mm/s)	914
Scan spacing (mm)	0.15
Layer thickness (mm)	0.1
Part bed temperature (°C)	177–178

The tensile, flexural, and compressive test specimens were prepared according to BS ISO references 527.2, 178, and 604, respectively, which correspond to ASTM D0638, D0790, and D0695 standards, respectively. The geometry and dimensions of tensile, compressive, and flexural test specimens are shown in Figure 1.

The tensile test specimens and the compressive test specimens were loaded at a speed of 5 mm/min while the loading rate at flexural test was 2 mm/min on specimens which spans 60 mm. For measuring the cross-sectional area of manufactured specimens, a micrometre was used; the average cross-sectional area of test specimens is necessary for evaluating the tensile and flexural properties. The dimensions were measured at least 3 times and an arithmetic average was calculated. The number and distribution of test specimens fabricated for this work are given in Table 4.

3. Results and Discussion

Objects in SLS process are built as a layer-by-layer, and consequently, it is expected to obtain inhomogeneous mechanical as well as morphological properties since the sintering conditions cannot be maintained identical throughout all the layers [8]. In the following sections, important fabrication parameters that may cause such inhomogeneities are investigated and their effects on the mechanical and morphological properties of manufactured SLS parts are evaluated. For this purpose, the effects of concerned fabrication parameters on ultimate tensile strength, compressive strength, flexural modulus are investigated; also, its effects on SLS part's surface quality are qualitatively evaluated. The results presented here were obtained at 10% weight fraction of white cement, and every plotted value is the arithmetic average of 5 readings; the reason for choosing such specific weight fraction of white cement is that it was reported by Aldahash [12] that at this weight fraction, optimal mechanical and morphological properties of cement-filled PA12 composite are obtained; Table 5 shows a comparison between the mechanical properties of PA12 and cement-filled PA12. The mechanical properties were investigated for specimens fabricated with three different values of laser power (i.e., 6, 7, and 8 watt) that result in EDs of 0.047, 0.051, and 0.054 J/mm^2, respectively. On the other hand, the surface quality was evaluated for specimens fabricated with values of laser power ranging from 4.5 to 8 watt.

3.1. Scanning Vector Length Effect. For the "DTM Sinterstation 2000" system, the SLS process is performed as follows: first, the laser scans the powder bed through scan paths (vectors) which are parallel to the x-axis (see Figure 2). Once the scanning path is completed, the laser head proceeds along the y-axis with a predetermined increment called the "scan spacing" and starts another scanning vector in the opposite direction.

Hence, as the laser head scans the powder layer along the x-direction, the laser energy heats the particles to the melting temperature of PA12 resulting in the formation of necks between adjacent particles, and hence strong bonds are formed between PA12 particles along the x-direction (see Figure 3(a)). However, while waiting for the next vector to be scanned, heat energy is released from previous scan path making the PA12 particles to cool down, and consequently, rather weak bonds are formed between beads of successive paths along the y-direction (see Figure 3(b)). Upon complete scanning, a fresh layer of powder is applied on top of the sintered and cooled layer, and hence the bonds between particles in consequent layer will be the weakest (see Figure 3(c)) [5]. Hence, based on the aforementioned discussion, the length of scanning vector is expected to have a significant effect on the mechanical properties of manufactured SLS specimens.

In order to investigate the effect of varying the scanning vector length on the mechanical properties of the SLS specimens, the parts were built along the orientations shown in Figure 4. The built specimens along the x-axis are entitled T1, C1, and F1 for tensile, compressive, and flexural testing, respectively, and a similar manner is used for naming the test specimens in other directions. As Figure 4 shows, for every layer, the laser head scans the object slice along the x-axis first and then proceeds along the y-direction.

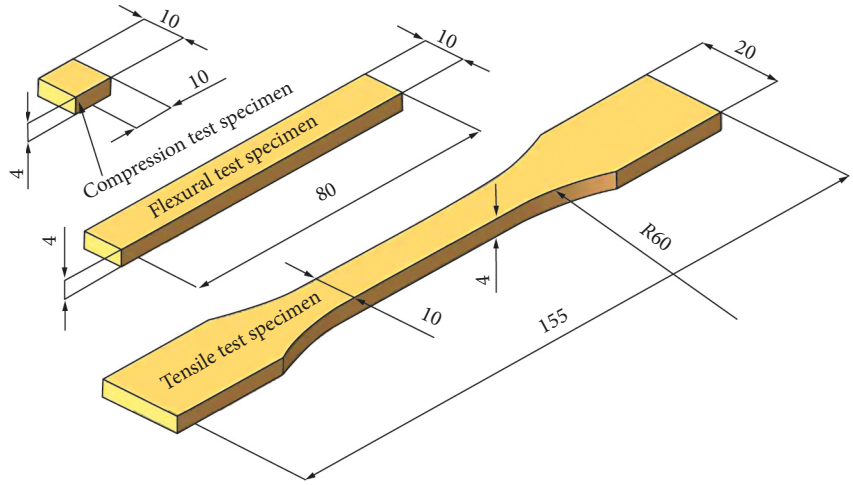

Figure 1: Geometry of tensile, compressive, and flexural test specimens.

Table 4: Number and distribution of test specimens.

	Tensile test	Flexural test	Compressive test
Laser power		3LPs (6, 7, and 8 watt)	
Orientations	3 orientations (T1, T2, and T3)	3 orientations (F1, F2, and F3)	2 orientations (C1 and C3)
Samples		5 specimens along each orientation	
Total	$3 \times 3 \times 5 = 45$ test specimens	$3 \times 3 \times 5 = 45$ test specimens	$3 \times 2 \times 5 = 30$ test specimens

Table 5: Comparison between the mechanical properties of PA12 and cement-filled PA12 (10% white cement, LP = 7 watt).

	PA12	Cement-filled PA12
Ultimate tensile strength (MPa)	49.49	50.6
Flexural modulus (GPa)	1.71	2.11
Flexural yield strength (MPa)	46.72	52.56
Compressive yield strength (MPa)	47	60.44

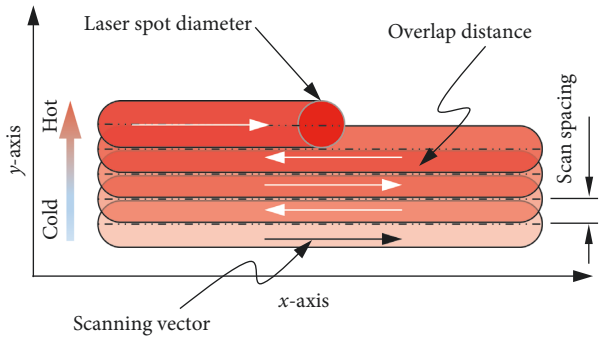

Figure 2: Scanning pattern of "DTM Sinterstation 2000" system.

The effect of scanning vector length on the ultimate tensile strength of cement-filled PA12 composite at laser power values of 6, 7, and 8 watt (i.e., ED = 0.047, 0.051, and 0.054 J/mm^2) and at 10% weight fraction of white cement is shown in Figure 5.

Although shorter scanning vector length is expected to result in strong bonding between PA12 particles and improved mechanical properties, the results from Figure 5 appear to contradict this conclusion; this is attributed mainly to the fact that the previous conclusion holds only if the tensile load acts along the direction of the scanning vector. Therefore, despite the tensile specimens T2 and T3 having shorter scanning vector length than that of T1, the direction of tensile load is normal to the scanning vector, and consequently, they possess lower ultimate tensile strength. In fact, the bonding between scanning paths is weaker than that along scanning direction, and hence the results from Figure 5 are consistent with previous explanation in Figure 3. Also, the results from Figure 5 are consistent with those reported by Gibson and Shi [6], Ajoku et al. [7], and Caulfield et al. [8]. Another interesting result from Figure 5 is that the tensile specimens which were built at laser power of 7 watt possess higher ultimate tensile strength compared with those built at other values of laser energy, and this conclusion holds for all lengths of the scanning vector; these results agree well with those reported by Aldahash [12].

Additionally, the effect of scanning vector length on the compressive strength of PA12/white cement composite is shown in Figure 6. Since the compressive test specimens have 10×10 mm square face, the specimen with C2 orientation is identical to that with C1 orientation; therefore, the effect of scanning vector length on only C1 and C3 specimens was investigated. It is apparent from the figure that the compressive strength of SLS parts increases with increasing the scanning vector length. Consistent with previous results, the specimens with 7 watt laser energy have the highest compressive strength regardless of the length of the scanning

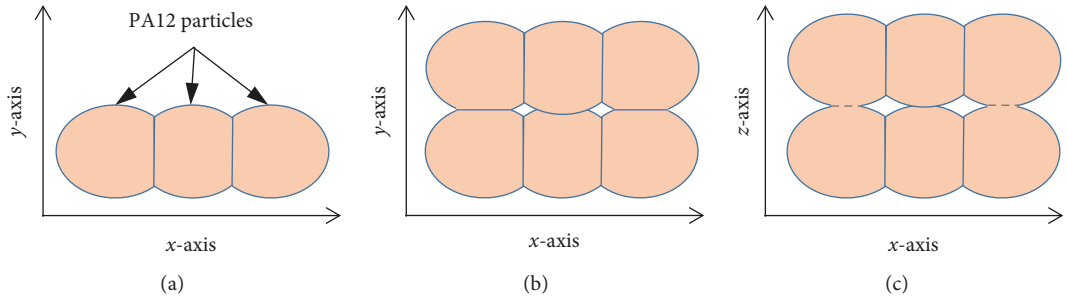

Figure 3: Schematics of bonding mechanism between PA12 particles in SLS: (a) strong bonds formed along the x-axis; (b) weak bonds between successive scan paths along the y-axis; (c) weakest bonds between layers along the z-axis.

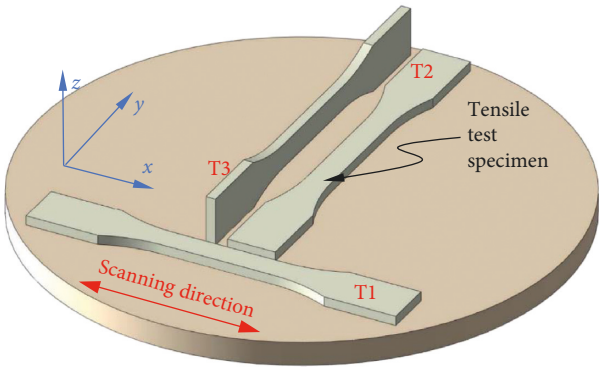

Figure 4: Orientations of tensile test specimens for different scanning vector lengths.

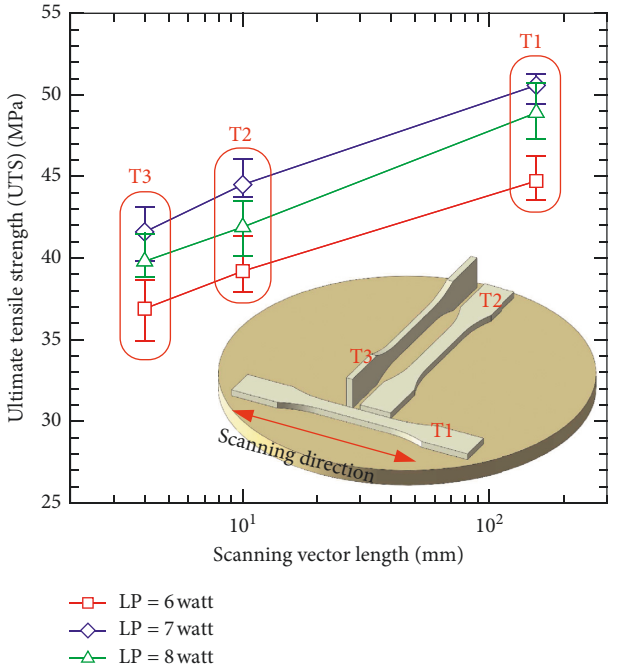

Figure 5: Effect of scanning vector length on ultimate tensile strength of PA12/white cement composite.

vector. The results from Figure 6 may be explained by considering the fact that failure in compressive test occurs mainly due to slipping between layers, and hence the test

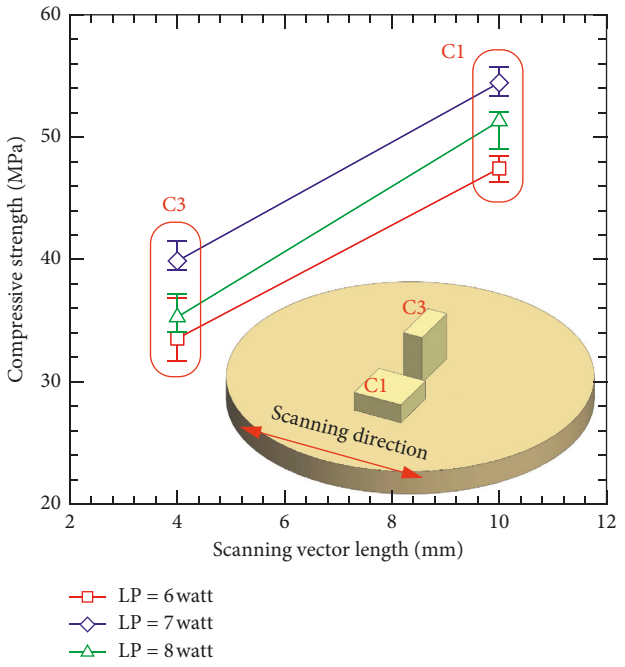

Figure 6: Effect of scanning vector length on the average compressive strength of PA12/white cement composite.

specimen with small number of layers (C1) is expected to have a higher compressive strength than that with large number of layers (C3).

Finally, the effect of scanning vector length on the flexural resistance of SLS PA12/white cement specimens is shown in Figure 7. It is noticeable for the results that the values of flexural modulus increase with increasing the length of scanning vector. Also, consistent with Aldahash [12], the results show that the specimens built at LP of 7 watt have higher flexural modulus than those built at either lower or higher LP values. Surprisingly, the flexural modulus of F2 parts is comparable to those of F1 parts, and at LP of 8 watt, the value of F2 flexural modulus is slightly higher than that of F1. This finding was also reported by Gibson and Shi [6] who found that shorter scan vectors result in uniform temperature during sintering process which in turn ensures strong bonds between successive scan vectors and particles in the same scan vector and

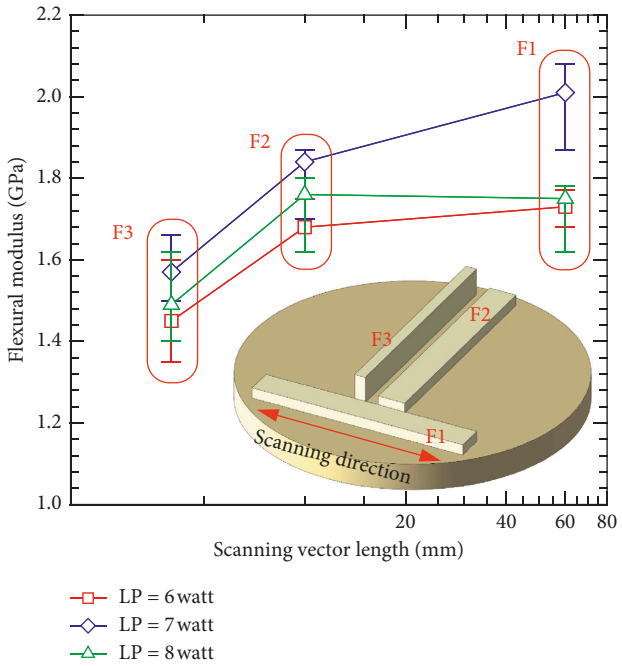

Figure 7: Effect of scanning vector length on the average flexural modulus of PA12/white cement composite.

consequently enhances the mechanical properties of manufactured SLS parts.

3.2. End-of-Vector (EOV) Effect. During the SLS process, as the head accelerates at the start of every scan vector, the layer edge is exposed to initial burst of laser that is slightly higher than the predetermined energy (see Figure 8). Such way of localized exposure to laser energy enhances melting and fusion of PA12 particles and, consequently, improves the mechanical properties at layer edges; however, excessive exposure may result in overheating and burning of SLS part's edge. It is extremely important to realize that this end-of-vector effect occurs only at edges normal to the scanning vector; Ajoku et al. [7] reported that EOV effect is most prominent in parts with small dimensions. Also, as the scanning head decelerates near the end of scanning path, the opposite edge of the layer is exposed to large amount of laser energy than the innermost particles.

Figure 9 shows SEM pictures describing the EOV effect on SLS parts manufactured at different values of laser power. As discussed previously, excessive exposure to laser energy at layer edges results in melting and viscous shear flow which in turn deteriorates the alignment of layer edge (see Figure 9(a)). Moreover, such localized heating results in burning of layer edges, which is manifested by the dark-colour edge (see Figure 9(b)), and can result in overheating and surface microcracks (see Figure 9(c)). On the other hand, the layer edge that is parallel to scanning direction does not suffer from such excessive exposure to laser energy; however, the round-shape of this edge is primarily due to the uneven cooling rate at layer edge (see Figure 9(d)).

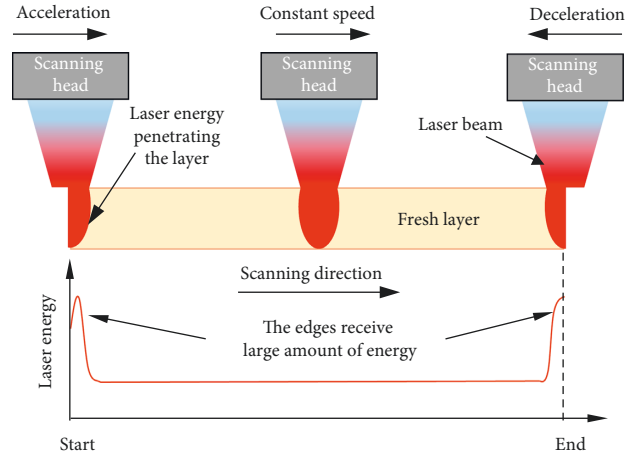

Figure 8: Schematics of the end-of-vector (EOV) effect in the SLS process.

3.3. Laser Power Effect on Surface Quality. The laser power has a significant effect on the surface quality of parts manufactured with SLS technology. This effect is better illustrated in Figures 10 and 11. Figure 10 shows the effect of incident laser power on the surface microstructure of PA12/white cement samples. At small values of LP (Figures 10(a) and 10(b)), the incident laser energy is not sufficient to penetrate the powder layer and efficiently melt the PA12 particles. As the laser power increases (Figure 10(c)), the resulting ED becomes sufficient to melt and fuse the PA12 particle together, resulting in homogeneous and smooth surface. However, further increase in the laser energy (Figure 10(d)) causes overhearing and surface microcracks; this finding was also reported by Caulfield et al. [8] and Dewidar [13].

The results from Figure 10 are further emphasized in Figure 11 which shows the effect of laser power on the surface topography of manufactured SLS parts. It is apparent from Figure 11 that increasing the energy density (ED) could enhance the surface roughness of manufacture parts; however, excessive increase in laser power causes localized burning and initiation of surface microcracks.

4. Conclusions

Selection of proper values of fabrication parameters in SLS process is inevitable in order to manufacture the objects as designed and free from apparent and hidden defects. For this purpose, the present experimental work is devoted to evaluating the effects of important fabrication parameters on the mechanical and morphological properties of cement-filled PA12 parts fabricated with SLS technique. The effects of scanning vector length on tensile, compressive, and flexural strength of manufactured parts were evaluated. Additionally, the end-of-vector (EOV) effect on part's edge geometry was evaluated. Also, the effect of laser power on the surface quality and surface finish was qualitatively evaluated. The most obvious findings to emerge from this study are as follows:

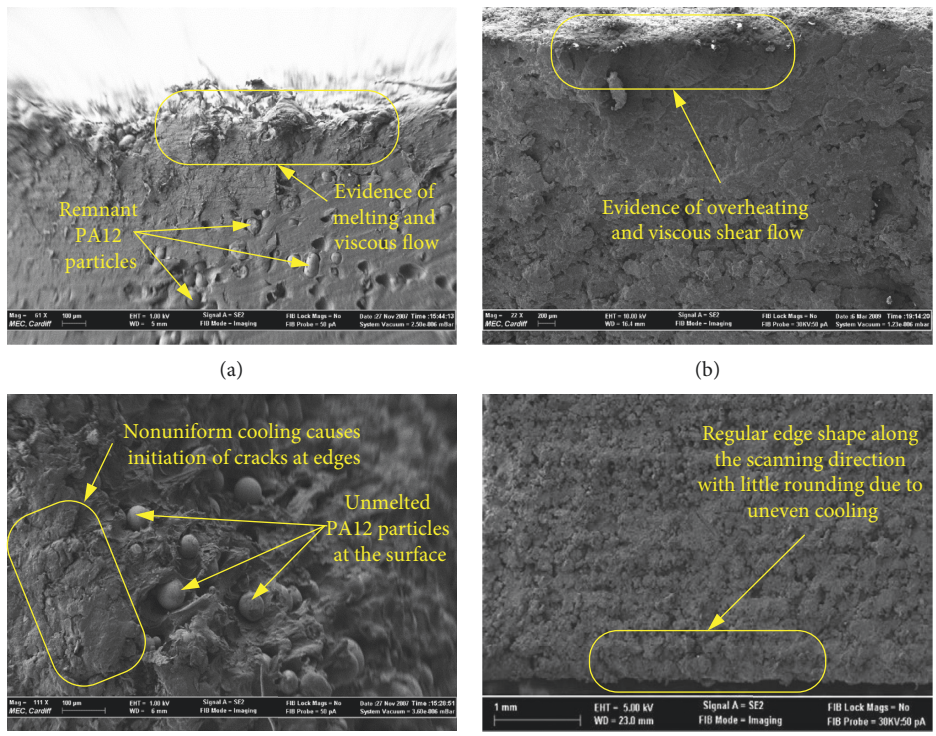

Figure 9: SEM micrograph showing the end-of-vector (EOV) effect in the SLS process; LP = 7 watt (ED = 0.051 J/mm^2) at 10% weight fraction of white cement.

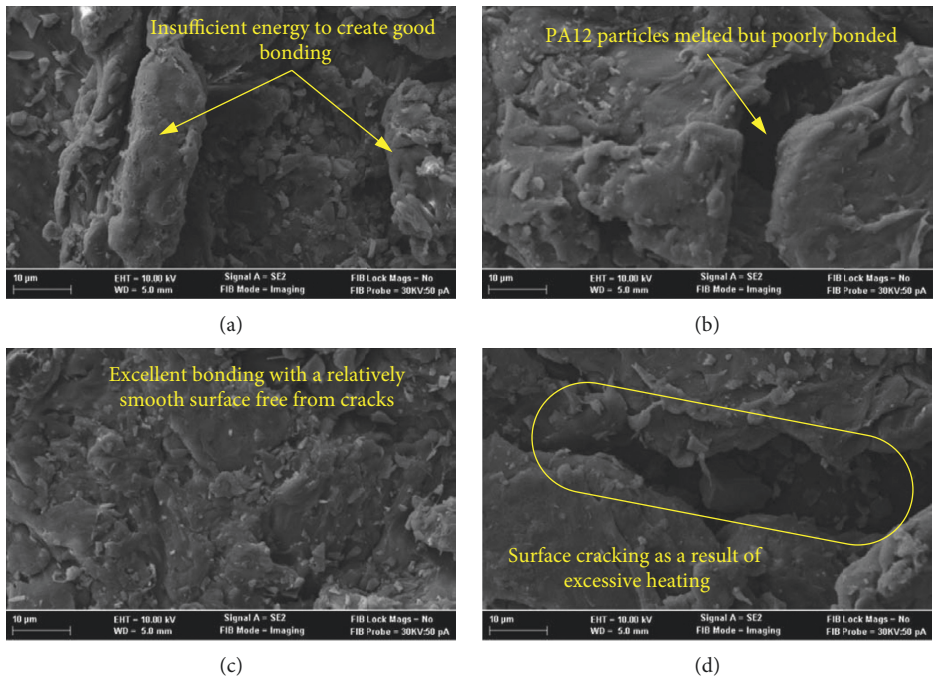

Figure 10: Effect of laser power on surface properties of SLS parts: (a) LP = 5.5 watt; (b) LP = 6.5 watt; (c) LP = 7.0 watt; (d) LP = 8.0 watt.

(i) Scanning vector length significantly affects the mechanical properties of SLS parts provided that the load is applied along the scanning vector direction.

(ii) Excessive exposure to laser energy at layer edges can result in viscous shear flow which in turn deteriorates the part edge and in some cases can cause localized heating which results in burning of layer

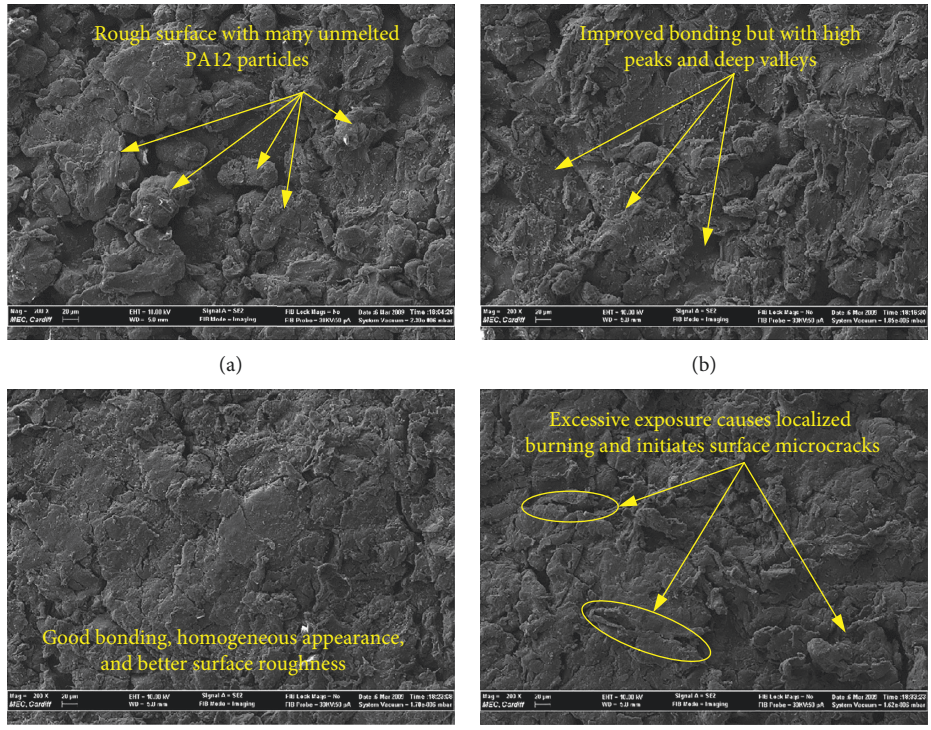

Figure 11: Effect of laser power on surface topography of SLS parts: (a) LP = 4.5 watt; (b) LP = 6.0 watt; (c) LP = 7.0 watt; (d) LP = 8.0 watt.

edges; in severe cases, EOV effect can result in overheating and surface microcracks.

(iii) Increasing the laser power could enhance the surface roughness of manufacture parts; however, excessive increase in laser power causes localized burning and initiation of surface microcracks.

(iv) The adopted hatching pattern (parallel to x-axis) at every layer contributes to the resulting anisotropy. Hence, in order to enhance the mechanical properties of parts fabricated with SLS process, it is recommended to rotate the hatching path at each layer relative to the hatching path of underneath sintered layer.

Data Availability

The experimental data used to support the findings of this study are included within the article.

Conflicts of Interest

The authors declare that there are no conflicts of interest regarding the publication of this paper.

Acknowledgments

The authors would like to thank Professor Duc Pham for the kind support through all the manufacturing processes at the Manufacturing Engineering Centre in Cardiff University (UK). The authors would like to thank the Deanship of Scientific Research at Majmaah University for supporting this work under Project no. 1440-45.

References

[1] T. L. Starr, T. J. Gornet, and J. S. Usher, "The effect of process conditions on mechanical properties of laser-sintered nylon," *Rapid Prototyping Journal*, vol. 17, no. 6, pp. 418–423, 2011.

[2] D. T. Pham and S. S. Dimov, *Rapid Manufacturing: The Technologies and Applications of Rapid Prototyping and Rapid Tooling*, Springer, London, UK, 2000.

[3] D. T. Pham and S. S. Dimov, "Rapid prototyping and rapid tooling—the key enablers for rapid manufacturing," *Proceedings of the Institution of Mechanical Engineers, Part C: Journal of Mechanical Engineering*, vol. 217, no. 1, pp. 1–23, 2003.

[4] N. Hopkinson, R. Hague, and P. Dickens, *Rapid Manufacturing: An Industrial Revolution for the Digital Age*, John Wiley & Sons, Ltd., Chichester, UK, 2006, ISBN: 0-470-01613-2.

[5] R. D. Goodridge, C. J. Tuck, and R. J. M. Hague, "Laser sintering of polyamides and other polymers," *Progress in Materials Science*, vol. 57, no. 2, pp. 229–267, 2012.

[6] I. Gibson and D. Shi, "Material properties and fabrication parameters in selective laser sintering process," *Rapid Prototyping Journal*, vol. 3, no. 4, pp. 129–136, 1997.

[7] U. Ajoku, N. Saleh, N. Hopkinson, R. Hague, and P. Erasenthiran, "Investigating mechanical anisotropy and end-of-vector effect in laser-sintered nylon parts," *Proceedings of the Institution of Mechanical Engineers, Part B: Journal of Engineering Manufacture*, vol. 220, no. 7, pp. 1077–1086, 2006.

[8] B. Caulfield, P. E. McHugh, and S. Lohfeld, "Dependence of mechanical properties of polyamide components on build

parameters in the SLS process," *Journal of Materials Processing Technology*, vol. 182, no. 1–3, pp. 477–488, 2007.

[9] W. Cooke, R. Anne Tomlinson, R. Burguete, D. Johns, and G. Vanard, "Anisotropy, homogeneity and ageing in an SLS polymer," *Rapid Prototyping Journal*, vol. 17, no. 4, pp. 269–279, 2011.

[10] S. K. Singhal, P. K. Jain, P. M. Pandey, and A. K. Nagpal, "Optimum part deposition orientation for multiple objectives in SL and SLS prototyping," *International Journal of Production Research*, vol. 47, no. 22, pp. 6375–6396, 2009.

[11] J. Bai, J. Song, and J. Wei, "Tribological and mechanical properties of MoS_2 enhanced polyamide 12 for selective laser sintering," *Journal of Materials Processing Technology*, vol. 264, pp. 382–388, 2019.

[12] S. A. Aldahash, "Optimum manufacturing parameters in selective laser sintering of PA12 with white cement additives," *The International Journal of Advanced Manufacturing Technology*, vol. 96, no. 1–4, pp. 257–270, 2018.

[13] M. A. Dewidar, *Direct and indirect laser sintering of metals*, The University of Leeds, Leeds, UK, Ph.D. thesis, 2002.